ESA contract
Martian Environmental Model

Ref : ESA 11369/95/NL/JG(SC)

WP5 deliverable :

Technical note on model validation

François Forget, Frédéric Hourdin, Christophe Hourdin, Steven Lewis, Frédéric Mathiot
LMD/AOPP

March 18, 1999

1 Introduction

This document briefly reviews the studies that have been performed to validate the LMD-AOPP Martian General Circulation model. It focusses on the studies carried out in the past two years, after the previous Work Packages which already included such model validation studies (see the technical reports entitled "Technical note on GCM testing" and "Sub-Grid Scale Orographic Parametetrisation Validation" delivered in May 1996, as well as the "Mars climate database v1.0 critical review" delivered in May 1997).

Originally, the purpose of the present document was to present the extension of the model validation based on the new observations which should have been gathered by Mars Pathfinder and especially Mars Global Surveyor. Unfortunately, because of the delay of the Mars Global Surveyor mission, detailed comparisons and validation with the MGS data have not yet been possible.

Nevertheless, several studies relevant to the validation of the model have been performed in the past years. In particular, many comparisons between the model outputs and the observations, along with some analysis of the zonal-mean fields simulated by the model were published in two article submitted to *Journal of Geophysical Research-planet* which are included in the appendix:

Paper 1: "Improved General Circulation Models of the Martian Atmosphere from the Surface to Above 80 km" (Forget et al. 1999).

Paper 2: "A Climate Database for Mars" (Lewis et al. 1999).

Other recent results are presented here. All these studies lead to an important conclusion concerning the dust radiative properties at solar wavelenghts, as explained in section 5.

2 Comparison with Viking

Comparison between the boundary layer scheme and the Viking Lander 1 observations of the diurnal variation of the wind velocities and turbulence are presented in Paper 1 , figure 3.

Paper 2 show some comparisons of the annual pressure cycle (Figures 7) and the entry temperature profile (figure 8) observed by the two landers and simulated by the model (as stored in the climate database).

Figure 1 and 2 of the present document show comparisons with the 15-μm Viking IRTM brightness temperature sampling the atmosphere around the 25-km level (see discussion in section 5)

3 Comparison with Pathfinder

The meteorological observations obtained by Pathfinder have been compared with the model simulation (as stored in the database). This include the surface observations of the diurnal cycle of surface pressure (Fig. 13 in Paper 2), near-surface temperature (Fig. 14 in Paper 2), and wind direction (Fig. 15 in Paper 2). In all theses cases, the agreement between data and model is extremely good.

Figure 12 in Paper 2 show the Pathfinder entry temperature profile. The agreement with the model simulation is not as spectacular, but it is acceptable to first order (see dicussion in the article). The simulated profiles shown in this figure were obtained using the original dust properties at solar wavelenght from Ockert-Bell et al. (1997) . Brighter dust properties provide a better agreement as shown in Figure 3 of the present document (see discussion in section 5).

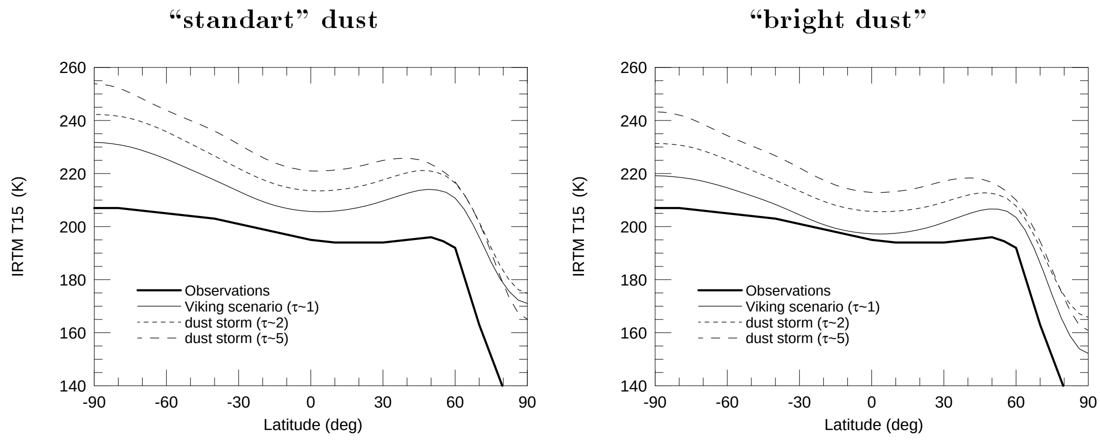

Figure 1: Comparison of the observed 15-μm Viking IRTM brightness temperature sampling the atmosphere around the 25-km level (averaged over $L_s = 250^o - 274^o$) with with those retrieved from the GCM (averaged over $L_s = 240 - 290^o$). Simulation carried out for various dust scenario and dust properties at solar wavelenght are presented (see text). The observed temperatures correspond to a period between 2 global dust storms, during which Viking Lander 1 measured a visble optical depth $\tau \simeq 1$.

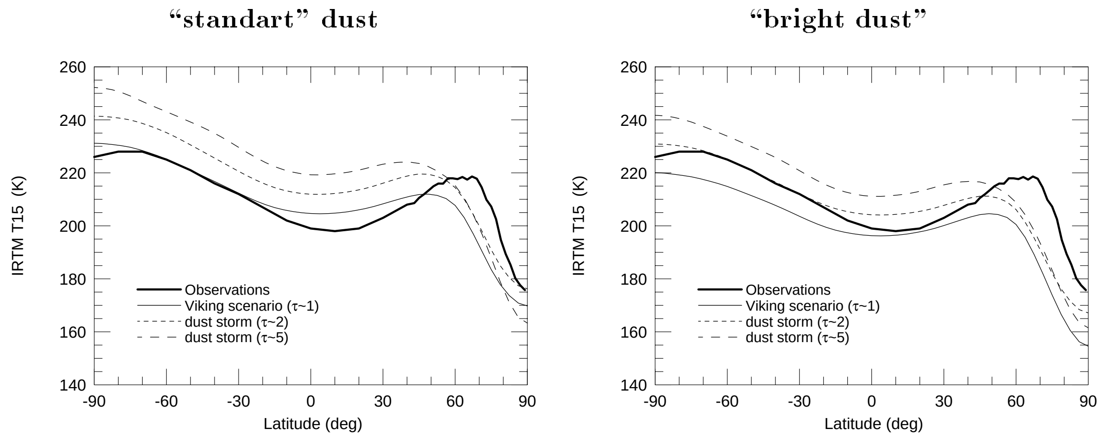

Figure 2: Same as Fig. 1 with observations averaged over $L_s = 274^o_2 90^o$ and simulations averaged over $L_s = 270 - 300^o$. The observed temperatures correspond to the peak of the second global dust storm during which Viking Lander 1 measured a visible optical depth τ between 2 and 4.

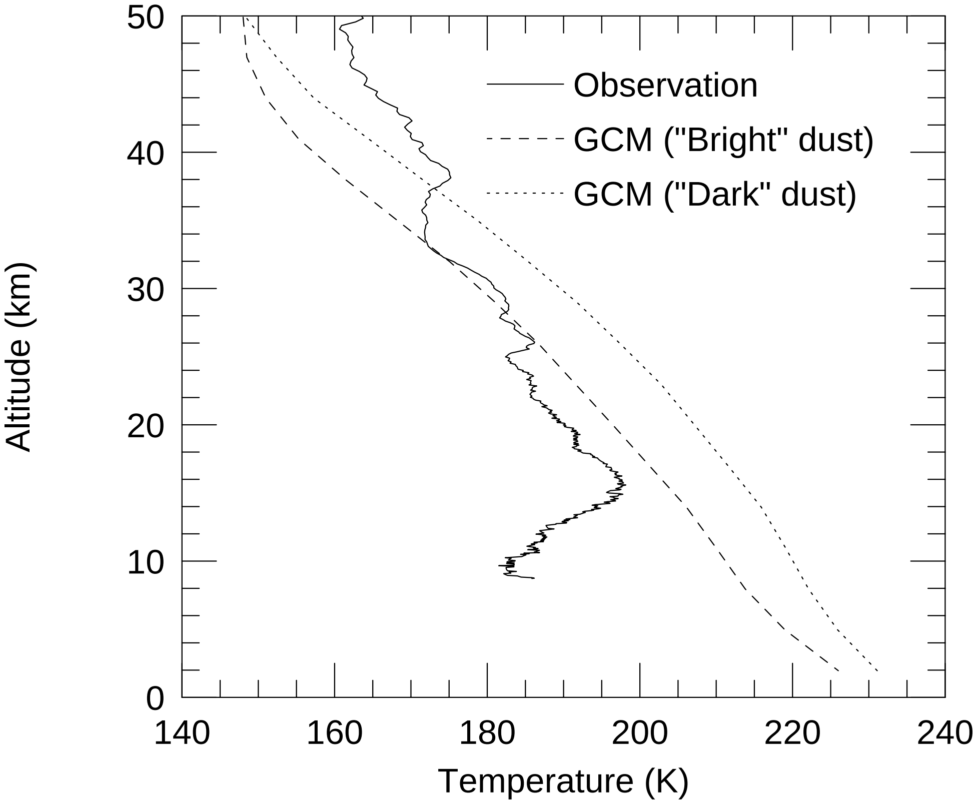

Figure 3: The temperature profile observed by Mars Pathfinder compared to corresponding model simulations obtained with the "dark" Ockert-Bell et al. (1997) and "bright" Clancy and Lee (1991) dust radiative properties at solar wavelenghts. The GCM use the "Viking year" dust distribution, which is though to accurately match the conditions observed by Pathfinder (Pathfinder camera observed Viking-like atmospheric opcaity shortly after landing, with $\tau_{vis} \simeq 0.4$). Data were kindly provided by J. A. Magalhaẽs from NASA Ames.

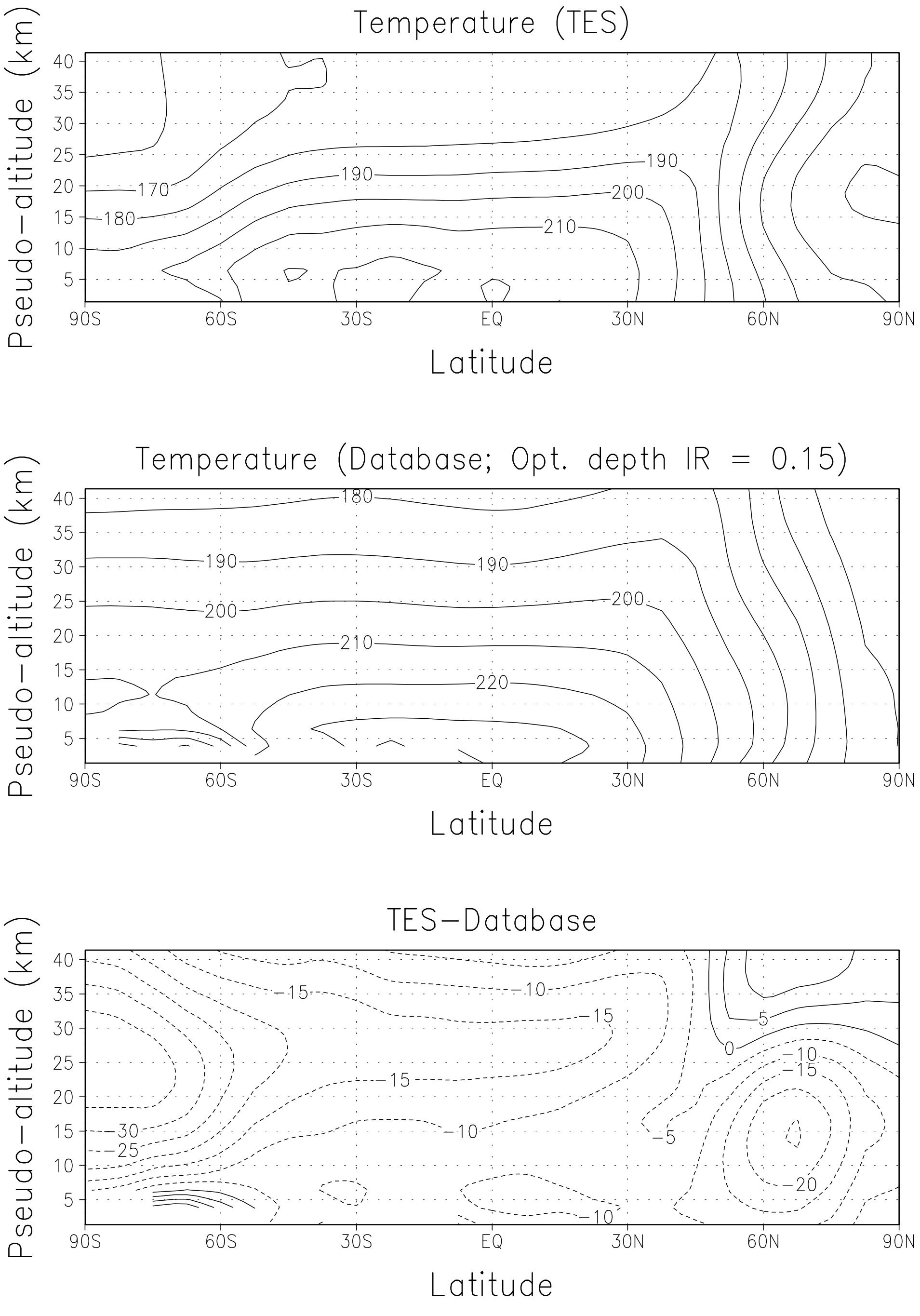

Figure 4: Time-mean section of zonal-mean temperature (K) as observed by the Thermal Emission Spectrometer aboard Mars Global Surveyor (November 1997, $L_s = 198^o - 213^o$) and simulated by the General Circulation Model for the same period and for a similar dust opacity ($\tau_{IR} = 0.15$ and $\tau_{vis} = 0.3$ at 700 Pa) with the **standart Ockert-Bell et al. (1997)'s dust radiative properties** at solar wavelenght. Data kindly provided by B. Conrath and J. Pearl from NASA GSFC.

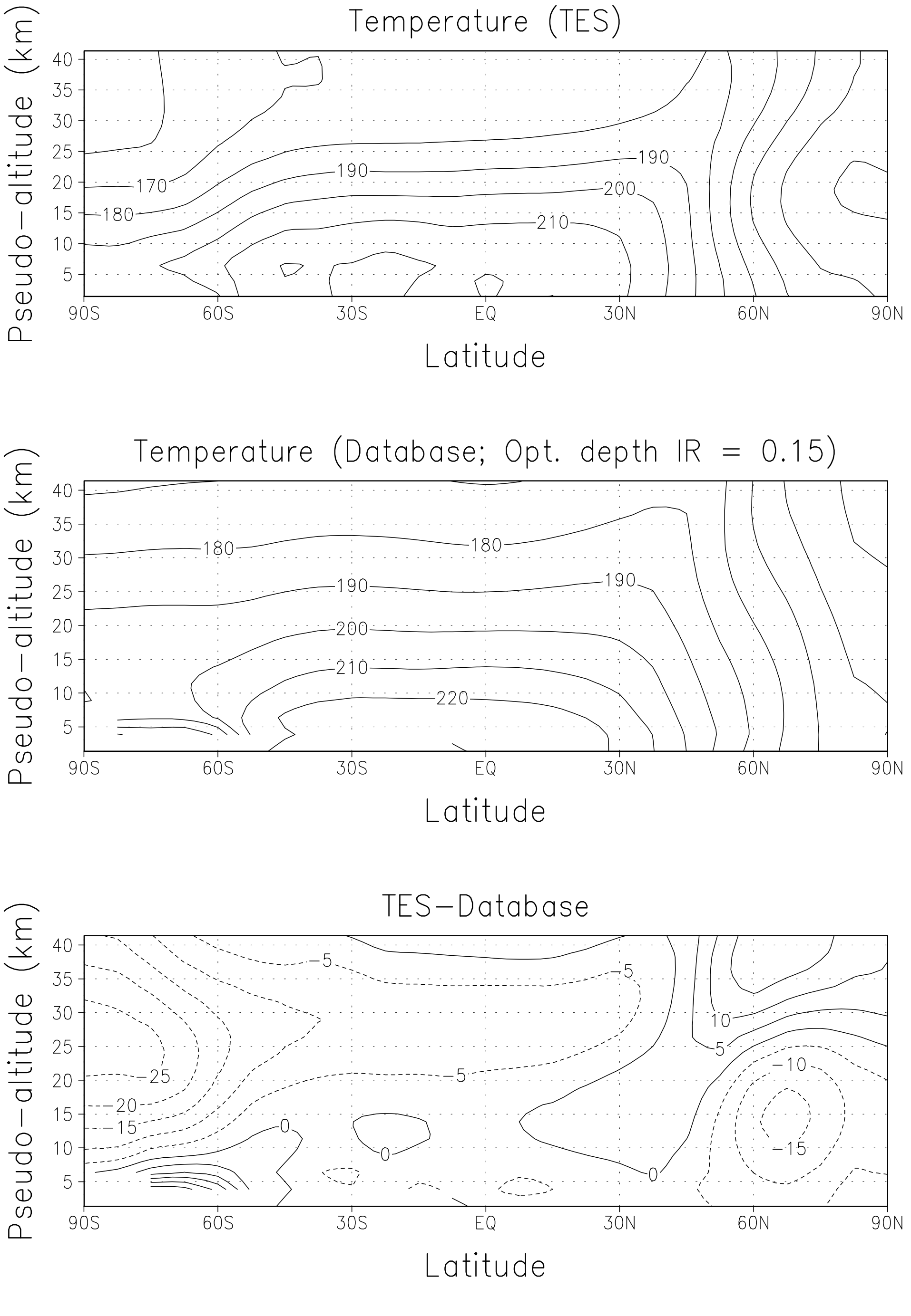

Figure 5: Same as Fig. 4 with the GCM using the **brighter Clancy and Lee (1991)'s dust radiative properties** at solar wavelenghts.

4 Comparison with Mars Global surveyor TES data

Temperature profiles obtained by inverting radiance spectra measured by the Thermal Emission Spectrometer (TES) during the "hiatus" of the aerobraking phase of MGS in november 1997 (see Christensen et al. 1998) have recently been made available to us by John Pearl and Barney Conrath from NASA-GSFC. Figure 4 and 5 show preliminary comparisons of the observed and simulated time-mean, zonal-mean temperature fields. The agreement is, to first order, acceptable. It depends on the chosen dust optical properties (see below) and it could be improved in the near future by using a dust spatial distribution closer to the actual conditions observed by Mars Global Surveyor at the time. For instance, differences in the dust distribution may explain the discrepancy between model and observations in the south polar region. Nevertheless, further studies using these data and other upcoming data will likely suggest some changes in the model parametrisations and model parameters in the future.

5 Alternative dust radiative properties at solar wavelenghts

Choosing accurate dust radiative properties to be used by the model at solar wavelenght remains a major issue. On the one hand, this is due to the fact that the dust single scattering properties may vary with altitude, season and horizontal locations, and that the various properties obtained by the different past studies may not be representative. In particular, it is likely that in some conditions, the dust particles can get coated by water ice. On the other hand, the radiative transfer results which are of importance for the GCM (e.g. heating rates) are unfortunately extremely sensitive to the dust properties. For instance, the dust single scattering albedo ω at solar wavelength is thought to be quite high, typically around 0.9. An uncertainty of $\pm 5\%$ then corresponds to an error on the heating rate of about $\pm 50\%$...

In the standart version of the model in the past years, we had chosen to use what is considered to be the most complete and acurate dataset currently available: the spectral single-scattering properties extrapolated over the solar wavelengths by Ockert-Bell et al. (1997) from the Pollack et al. (1995) Viking Lander data. These data appears to be consistent with the more recent Pathfinder observations (Markiewicz et al., 1999). However, Alternative dust properties have been proposed by Clancy and Lee (1991) on the basis of their analysis of the Viking orbiter infrared thermal mapper (IRTM) emission-phase-function measurements. These observations, performed from above the atmosphere rather than from Landers in the case of the studies previously mentionned, yield brighter dust properties, with a higher single scattering albedo and a lower asymetry parameter (See table 1 in paper 1).

We have found that using these properties corresponding to a "brighter" dust (and thus to an atmosphere about 10 K colder around 10 to 20 km) allowed the model to obtain temperature systematically closer to the observations. In practice, this conclusion was reached by looking at several datasets, including:

- **Viking IRTM brightness temperatures.** The IRTM instrument 15-μm channel measured the atmospheric temperature over a broad altitude range with maximum sensitivity around 25 km altitude. Simulated IRTM 15-μm temperature from the GCM were found to be systematically 10 to 20 K warmer than the observations at sunlit latitudes when using the Ockert-Bell (1997)'s radiative properties Figure 4 and 5 show such comparisons performed before and during the second global dust storm observed by Viking. It clearly appears that the model is closer to the observations when using Clancy and Lee's "bright" dust properties.

- **Pathfinder entry profile.** Figure 3 show a comparison of the observed entry profile with simulated profiles obtained with both dust radiative properties. Clancy and Lee (1991)'s brighter dust allows a much better agreement between 15 and 45 km. Below 15 km, the observed thermal inversion is thought to be due to a water ice cloud which cannot be simulated by the model. Above 45 km, the dust mixing ratio is low, the heating rates due to dust is small, and the thermal structure is probably controlled by dynamical processes.

- **Mars Global Surveyor TES temperatures.** Figures 4 and 5 clearly show a better agreement when using the brighter dust properties, especially at sunlit latitudes.

Until more data are available to improve our understanding of the model behavior and its ability to reproduce the actual Martian atmosphere, we suggest to use Clancy and Lee (1991)'s brighter dust properties for the model and the database.

References

Christensen, P. R., Anderson, D. L., Chase, S. C., Clancy, R. T., Clark, R., Conrath, B. J., Kieffer, H. H., Kuzmin, R. O., Malin, M. C., Pearl, J. C., Roush, T. L., and Smith, M. D. (1998). Results from the Mars Global Surveyor Thermal Emission Spectrometer. *Science*, 279:1692–1698.

Clancy, R. T. and Lee, S. W. (1991). A new look at dust and clouds in the Mars atmosphere: analysis of emission-phase function sequences from global Viking IRTM observations. *Icarus*, 93:135–158.

Forget, F., Hourdin, F., Fournier, R., Hourdin, C., Talagrand, O., Collins, M., Lewis, S. R., Read, P. L., and Huot., J.-P. (1999). An improved general circulation model of the Martian atmosphere from the surface to above 80 km. Submitted to J.G.R.

Lewis, S. R., Collins, M., Read, P. L., Forget, F., Hourdin, F., Fournier, R., Hourdin, C., Talagrand, O., and Huot., J.-P. (1999). A climate database for Mars. Submitted to J.G.R.

Markiewicz, W. J., Sablotny, R. M., Keller, H. U., Thomas, N., Titov, D., and Smith, P. H. (1999). Optical properties of the Martian aerosols as derived from Mars Pathfinder midday sky brightness data. *JGR planet*, in press, 1999.

Ockert-Bell, M. E., Bell III, J. F., McKay, C., Pollack, J., and Forget, F. (1997). Absorption and scattering properties of the Martian dust in the solar wavelengths. *J. Geophys. Res.*, 102:9039–9050.

Pollack, J. B., Ockert-Bell, M. E., and Shepard, M. K. (1995). Viking Lander image analysis of Martian atmospheric dust. *J. Geophys. Res.*, 100:5235–5250.